Molecular Pharmacology Fast Forward. Published on October 21, 2009 as doi:10.1124/mol.109.059931
This article has not been copyedited and formatted. The final version may differ from this version.

MOL#59931

Mechanisms of inhibition of T-type calcium current in the reticular thalamic neurons by 1-octanol: implication of the protein kinase C pathway

Pavle M. Joksovic, Won Joo Choe, Michael T. Nelson, Peihan Orestes, Barbara C. Brimelow and Slobodan M. Todorovic

Departments of Anesthesiology (PMJ, WJC, PO, MTN, BCB, SMT),

Neuroscience (SMT) and Neuroscience Graduate Program (PO, SMT)

University of Virginia Health System, Charlottesville, VA;

(PMJ present address) Department of Psychiatry, Yale University, 300 George St. Suite 901, New Haven CT 06511

(WJC present address) Department of Anesthesiology, InJe University, Ilsan Paik Hospital & College of Medicine, Goyang-city 411-706, Gyunggi-do, South Korea

Molecular Pharmacology Fast Forward. Published on October 21, 2009 as DOI: 10.1124/mol.109.059931
This article has not been copyedited and formatted. The final version may differ from this version.

RUNNING TITLE PAGE

a) Running title: 1-octanol inhibits T-current in the thalamus

b) Correspondence to Slobodan M. Todorovic
Department of Anesthesiology, University of Virginia Health System,
Mail Box 800710, Charlottesville, VA 22908-0710
Phone 434-924-2283
Fax 434-982-0019
Email:st9d@virginia.edu

c) Number of figures: 6
Number of tables: 0
Number of text pages: 31
Number of references: 37
Number of words in Abstract: 232
Number of words in Introduction: 397
Number of words in Discussion: 1145

d) Abbreviations:

LTS (low threshold spike)
DRG (dorsal root ganglion)
LVA (low-voltage-activated)
nRT (reticular thalamic nucleus)
LRR (loss of righting reflex)
TEA (tetraethylammonium)
HEK (human embryonic kidney)
TMA-OH (tetramethylammonium hydroxide)
PMA (phorbol 12-myristate 13-acetate)
4α-PMA (4α-phorbol 12-myristate 13-acetate)
Go 6976 (12-(2-cyanoethyl)-6,7,12,13-tetrahydro-13-methyl-5-oxo-^{5}*H*-indolo(2,3-a)pyrrolo(3,4-c)-carbazole)
TTX (tetrodotoxin)
PKC (protein kinase C)
DMSO (dimethylsulfoxide)
BAPTA (1,2-bis(o-aminophenoxy)ethane-N,N,N',N'-tetraacetic acid)
EGTA (ethylene glycol tetraacetic acid)

Molecular Pharmacology Fast Forward. Published on October 21, 2009 as DOI: 10.1124/mol.109.059931
This article has not been copyedited and formatted. The final version may differ from this version.

ABSTRACT

Recent studies indicate that T-type calcium channels (T-channels) in the thalamus are cellular targets for general anesthetics. Here, we recorded T-currents and underlying low-threshold calcium spikes from neurons of nucleus reticularis thalami (nRT) in brain slices from young rats and investigated the mechanisms of their modulation by an anesthetic alcohol, 1-octanol. We found that 1-octanol inhibited native T-currents at subanesthetic concentrations with an IC_{50} of about 4 μM. In contrast, 1-octanol was up to 30-fold less potent in inhibiting recombinant $Ca_V3.3$ T-channels heterologously expressed in human embryonic kidney (HEK) cells. Inhibition of both native and recombinant T-currents was accompanied by a hyperpolarizing shift in steady-state inactivation indicating that 1-octanol stabilized inactive states of the channel. To explore the mechanisms underlying higher 1-octanol potency in inhibiting native nRT T-currents, we tested the effect of protein kinase C (PKC) activator, phorbol 12-myristate 13-acetate (PMA) and PKC inhibitors. We found that PMA caused a modest increase of T-current while the inactive PMA analog, 4α-PMA failed to affect T-current in nRT neurons. In contrast, Go 6976, an inhibitor of calcium-dependent PKC, decreased baseline T-current amplitude in nRT cells and abolished the effects of subsequently applied 1-octanol. The effects of 1-octanol were also abolished by chelation of intracellular calcium ions with BAPTA. Taken together, these results suggest that inhibition of calcium-dependent PKC signaling is a possible molecular substrate for modulation of T-channels in nRT neurons by 1-octanol.

Molecular Pharmacology Fast Forward. Published on October 21, 2009 as DOI: 10.1124/mol.109.059931
This article has not been copyedited and formatted. The final version may differ from this version.

INTRODUCTION

Multiple subtypes of neuronal voltage-gated Ca^{2+} channels have a key function in controlling cellular excitability and transmitter release. The proposed functions of low-voltage-activated (LVA) or transient (T-type) Ca^{2+} channels (T-channels) include promotion of Ca^{2+}-dependent burst firing, generation of low-amplitude intrinsic neuronal oscillations, elevation of Ca^{2+} entry, and boosting of dendritic signals. These functions of T-currents in thalamic circuitry may contribute to pacemaker activity, wakefulness and sleep cycles, and seizure susceptibility (Llinas, 1988; Perez-Reyes, 2003). We have previously shown that volatile general anesthetics at clinically relevant concentrations block recombinant and native T-current variants in peripheral and central neurons (Todorovic and Lingle 1998; Todorovic et al., 2000; Joksovic et al., 2005a, 2005b). T-channels are abundantly expressed in thalamic nuclei, where they are crucial in control of the functional states of those neurons (McCormick and Ball, 1997; Llinas et al., 1999). Furthermore, inhibition of thalamic signaling has been implicated as a possibly common mechanism that contributes to such clinical effects of anesthetics as loss of consciousness and sedation (Rudolph and Antkowiak, 2004; Alkire, 2000). Therefore, the potential function of T-channels in the thalamus as targets for the action of general anesthetics remains an important issue in our understanding of the cellular mechanisms of anesthetic action.

Many normal alcohols have anesthetic capacity and are widely used to probe for molecular targets of anesthesia. Of particular interest for our studies is 1-octanol, which is a general anesthetic with estimated aqueous concentration EC_{50} values for loss of righting reflex (LRR) in tadpoles ranging from 57-130 μM (Alifimoff et al., 1989). Within the same range of concentration, 1-octanol may potentiate $GABA_A$-receptor-gated currents, one of the major cellular targets of general anesthesia (Franks and Lieb, 1994).

Molecular Pharmacology Fast Forward. Published on October 21, 2009 as DOI: 10.1124/mol.109.059931
This article has not been copyedited and formatted. The final version may differ from this version.

However, 1-octanol within the same concentration range also inhibits T-current in native systems, including adult dorsal root ganglion (DRG) cells (Todorovic and Lingle, 1998), GH_3 cell lines (Herrington and Lingle, 1992), hippocampal neurons (Takahashi et al., 1989), and thalamic relay neurons (Llinas et al., 2007). Moreover, we have demonstrated that 1-octanol blocks completely recombinant $Ca_V3.1$ (α1G) and $Ca_V3.2$ (α1H) T-channels, with estimated IC_{50} of 160 μM and 220 μM, respectively (Todorovic et al., 2000). Given the proposed importance of the thalamus in sensory processing and anesthetic states, we examined the effect of 1-octanol, a representative anesthetic alcohol, on T-current and underlying low-threshold Ca^{2+} spikes (LTS) in the reticular thalamic nucleus (nRT), the main inhibitory structure in the thalamus.

MATERIALS AND METHODS

***In vitro* tissue slice preparation.** We did most of these experiments on transverse rat brain slices cut through the middle anterior portion of the nRT (Paxinos and Watson 1982) at a thickness of 250-300 μm, as we have done previously (Joksovic et al., 2005a, 2005b,2006,2007). Gravid Sprague-Dawley rats were housed in a local animal facility in accordance with protocols approved by the University of Virginia Animal Use and Care Committee. We adhered to the guidelines in the *NIH Guide for the Care and Use of Laboratory Animals*.

Rats of either sex at the ages of 7-14 days were anesthetized with isoflurane and decapitated. The brains were rapidly removed and placed in chilled (4^{o}C) cutting solution consisting, in mM, of 2 $CaCl_2$, 260 sucrose, 26 $NaHCO_3$, 10 glucose, 3 KCl, 1.25 NaH_2PO_4, and 2 $MgCl_2$ equilibrated with a mixture of 95% O_2 and 5% CO_2. We glued a block of tissue containing the thalamus to the chuck of a vibrotome (WPI, Saratoga, FL) and cut slices in a transverse plane. We incubated the slices in 36^o C oxygenated saline

Molecular Pharmacology Fast Forward. Published on October 21, 2009 as DOI: 10.1124/mol.109.059931
This article has not been copyedited and formatted. The final version may differ from this version.

for 1 hr, then placed them in a recording chamber that was superfused at a rate of 1.5 cc/min with, in mM, 124 NaCl, 4 KCl, 26 $NaHCO_3$, 1.25 NaH_2PO_4, 2 $MgCl_2$, 10 glucose, and 2 $CaCl_2$ equilibrated with a mixture of 95% O_2 and 5% CO_2. Slices were maintained in the recording chamber at room temperature on room air, where they remained viable for at least 1 hour.

Recording procedures. The extracellular saline solution typically used for recording in voltage-clamp and current-clamp experiments consisted, in mM, of 2 $CaCl_2$, 130 NaCl, 2.5 $MgCl_2$, 10 glucose, 26 $NaHCO_3$, 1.25 NaH_2PO_4, and 0.001 tetrodotoxin (TTX). This was equilibrated with a mixture of 95% O_2 and 5% CO_2 for at least 30 minutes with final pH of 7.35-7.45. In some current-clamp experiments, TTX was omitted in order to study spike firing of nRT neurons. For recording T-currents in brain slices, we used an internal solution of, in mM, 135-140 tetramethylammonium hydroxide (TMA-OH), 10 EGTA, 40 HEPES, and 2 $MgCl_2$ titrated to pH 7.15-7.25 with hydrofluoric acid (HF) (Todorovic and Lingle 1998). In some experiments, we altered this internal solution by substituting BAPTA for EGTA. Recording electrodes for current-clamp studies contained, in mM, 130 KCl, 5 $MgCl_2$, 1 EGTA, 40 Na-HEPES, 2 MgATP, and 0.1 Na_3-GTP at pH 7.2. For the data presented, membrane potential values were not corrected for the measured liquid junction potential of -10 mV in voltage-clamp experiments or for the potential of -5 mV in current-clamp experiments.

All recordings were obtained from thalamic neurons visualized with an infrared differential interference contrast camera (C2400; Hammamatsu, Hammamatsu City, Japan) on the Zeiss 2 FS Axioscope (Jena, Germany) with a 40X lens and patch-clamp pipette using a Sutter micromanipulator MP-285 (Sutter Instrument, Novato, CA).

Recombinant human embryonic kidney (HEK) cells. HEK 293 cells were stably transfected with rat α1Ib ($Ca_V3.3.b$) constructs as described previously (Murbartian et al., 2002; Joksovic et al., 2005a). Cells were typically used 1 to 2 days

Molecular Pharmacology Fast Forward. Published on October 21, 2009 as DOI: 10.1124/mol.109.059931
This article has not been copyedited and formatted. The final version may differ from this version.

after plating. The standard extracellular saline for recording Ca^{2+} current contained (in mM) 160 TEA-Cl, 10 HEPES, and 2 $CaCl_2$, adjusted to pH 7.4 with TEA-OH. The internal solution consisted of (in mM) 110 Cs-methane sulfonate, 14 phosphocreatine, 10 HEPES, 1 or 9 EGTA, 5 Mg-ATP, and 0.3 Tris-GTP; the pH was adjusted to 7.15 to 7.20 with CsOH (standard osmolarity: 300 mOsm). All recordings of currents from HEK 293 cells were done using an inverted Zeiss 200 Axiovert microscope (Jena, Germany) with a 40X lens.

Electrophysiological recordings. Recordings were made with standard whole-cell voltage-clamp technique (Hamill et al., 1981). Electrodes were fabricated from thin-walled microcapillary tubes (Drummond Scientific, Broomall, PA) and had final resistances of 3-6 MΩ. We recorded membrane currents with an Axoclamp 200B patch-clamp amplifier (Molecular Devices, Foster City, CA). Voltage commands and the digitization of membrane currents were done with Clampex 8.2 of the pClamp software package (Molecular Devices, Foster City, CA). Neurons were typically held (V_h) at -90 mV and depolarized to test potential (V_t) of -50 mV every 10-20 seconds to evoke inward Ca^{2+} currents. Data were analyzed using Clampfit (Molecular Devices) and Origin 7.0 (OriginLab Corp, Northampton, MA). We filtered currents at 5-10 kHz and typically compensated for 50%-80% of series resistance (R_s). In most experiments, a P/5 protocol was used for on-line leakage subtraction.

Analysis of current inhibition. The percent reduction in peak T-current at a given 1-octanol concentration was used to generate concentration-response curves. For each such curve, all points are averages of multiple determinations obtained from at least five different cells. In most of the recombinant cells, we tested at least 2 different concentrations of 1-octanol, while in intact brain slices only one concentration was used per cell in a given slice. On all plots, vertical bars indicate standard errors of the means

Molecular Pharmacology Fast Forward. Published on October 21, 2009 as DOI: 10.1124/mol.109.059931
This article has not been copyedited and formatted. The final version may differ from this version.

(S.E.M). Mean values on concentration-response curves were fit to the following function:

$PB([1\text{-octanol}]) = PB_{max}/ (1+(IC_{50}/[1\text{-octanol}])^{n})$

where PB_{max} is the maximal percent inhibition of peak T-current, IC_{50} is the concentration that produces 50% of maximal inhibition, and *n* is the apparent Hill coefficient for inhibition. Fitted values are typically reported with 95% linear confidence limits.

Analysis of current. The voltage dependence of steady-state activation was described with a single Boltzmann distribution:

$$G(V) = G_{max}/(1+\exp[-(V-V_{50})/k])$$

where G_{max} is the maximal estimated conductance, V_{50} is the half-maximal voltage, and *k* (units of mV) represents the voltage dependence of the distribution. The voltage-dependence of steady-state inactivation was described with a single Boltzmann distribution:

$$I(V) = I_{max}/(1+\exp[(V-V_{50})/k])$$

where I_{max} is the maximal current, V_{50} is the half-maximal voltage, and *k* (units of mV) represents the voltage dependence of the distribution. The time course of current inactivation was fitted using a single exponential equation, $f(t) = A_1\exp(-t/\tau 1)$, yielding one-time constants (τ_1) and their amplitude (A_1).

For all current-voltage (I-V) curves and steady-state inactivation curves, fitted values typically were reported with 95% linear confidence limits. Input resistance (R_{in}) was determined from the slope of the peak voltage versus the current plot that resulted from injecting 80-160 msec-long current ranging from 100-1000 pA. Statistical analysis was performed with either Paired Student *t*-test or Unpaired Student *t*-test where appropriate, with statistical significance at $p < 0.05$.

Methodological considerations relevant to intact brain slices.

Molecular Pharmacology Fast Forward. Published on October 21, 2009 as DOI: 10.1124/mol.109.059931
This article has not been copyedited and formatted. The final version may differ from this version.

Recordings from intact brain slices offer great advantages for studying neurons in an intact setting *in vitro*. However, since voltage control is compromised in whole-cell recordings from slices due to the presence of extensive cell processes, we paid close attention to the signs of good voltage control. Specifically, there was no extensive delay in the onset of current; also, the onset and offset kinetics depended on voltage, not on the amplitude of current. In whole-cell experiments, because intact nRT neurons have long processes, rapid components of recorded current, such as fast-activation kinetics or tail currents, are not likely to reflect the true amplitude and time course of Ca^{2+} current behavior. All our measurements of amplitudes from holding, peak, and steady-state currents were made at time points sufficient to ensure reasonably well-clamped current conditions. Furthermore, using brain slices from young animals, in which dendrites are not fully developed, alleviated the space-clamp problem.

To facilitate application of drugs, we applied first 10 cc of external solution containing drug with bath flow of about 5 cc/minute, and then continued with perfusion of 1-2 cc/minute. All drugs were applied until an apparent steady-state effect on peak T-current was achieved. To avoid the accumulation of highly lypophilic substance in the tissue, we used only a single application of any given concentration of 1-octanol per slice.

Drugs and chemicals. Tetrodotoxin (TTX) was obtained from Alomone Lab (Jerusalem, Israel). All other salts and chemicals were obtained from Sigma Chemical (St. Louis, MO). Stock solutions (100 μM) of phorbol 12-myristate 13-acetate (PMA) and its inactive stereoisomer (4αPMA), as well as 12-(2-cyanoethyl)-6,7,12,13-tetrahydro-13-methyl-5-oxo-^{5}*H*-indolo(2,3-a)pyrrolo(3,4-c)-carbazole (Go 6976) at 10 mM, were made in dimethylsulfoxide (DMSO), while a 100 μM stock solution of TTX was prepared in distilled water. The maximal final concentration of DMSO used in our experiments was

Molecular Pharmacology Fast Forward. Published on October 21, 2009 as DOI: 10.1124/mol.109.059931
This article has not been copyedited and formatted. The final version may differ from this version.

0.1%, which does not significantly affect native thalamic Ca^{2+} currents (Joksovic et al., 2005a,b).

Solutions. Multiple independently controlled glass syringes attached to the common PVC tubing served as reservoirs for a gravity-driven perfusion system. Manually controlled valves were used to switch solutions. All experiments were done at room temperature (20-24^{o}C). All drugs were prepared as stock solutions kept in sealed glass vials and freshly diluted to appropriate concentrations as needed. 1-octanol was prepared from 2 mM stock solution obtained by mixing and stirring for several hours of 7.87 μL of 1-octanol with 25 cc of external solution in a sealed glass container. Aliquots of 1-octanol stock were then diluted to final concentrations and used fresh for each application. Determination of actual concentrations of 1-octanol in external solution was not performed. However, previous measurements with gas chromatography have indicated that the rate of volitalization of 1-octanol is less than 30% during first 2 hours of stock preparation (Lingle and Todorovic, personal communication). During each experiment, solution was removed from the end of the chamber opposite the tubing by constant suction. Changes in Ca^{2+} current amplitude in response to applied drugs or ionic changes typically were complete in up to 3 min. Switch of flow between separate perfusion syringes, each containing control saline, resulted in no significant changes in the amplitude and kinetics of T-current.

RESULTS

Bath application of 1-octanol potently inhibited T-current in nRT cells in brain slices that display characteristic slowly inactivating kinetics (Joksovic et al., 2005a; 2005b). Figure 1A shows traces and Figure 1B depicts the time course from the same voltage-clamp experiment in which 10 μM 1-octanol reversibly inhibited about 80% of the

Molecular Pharmacology Fast Forward. Published on October 21, 2009 as DOI: 10.1124/mol.109.059931
This article has not been copyedited and formatted. The final version may differ from this version.

peak T-current without an apparent effect on macroscopic current inactivation kinetics. Figure 1C summarizes average data points with 1, 3, 5, and 10 μM 1-octanol demonstrating concentration-dependent, potent, and almost complete inhibition of T-current. The solid line represents a Hill plot giving an estimated IC_{50} of about 4 μM.

We hypothesized that 1-octanol may abolish LTS of nRT neurons that critically depend on T-channels. Thus, we used current-clamp recordings from these cells and assessed spike firing when the neuronal membrane was depolarized with current injections through the recording electrode from holding negative membrane potentials (e.g., -90 mV), which maximize the availability of T-channels. Figure 2A presents traces from a representative nRT cell before, during, and after the application of 10 μM 1-octanol. 1-octanol reversibly depressed the number of action potentials that crowned LTS from 4 to 1. The histograms in Figure 2B indicate that in similar current-clamp experiments 10 μM 1-octanol significantly decreased the membrane firing that accompanied LTS from about 5 to 3 action potentials ($n = 6$ cells, $p < 0.05$). Even though in most of the cells applications of 1-octanol in current-clamp experiments caused changes in baseline membrane potential, overall average changes did not significantly differ between baseline (-54.3 ± 3.2 mV) and 1-octanol (-51.0 ± 5.3 mV , $n = 6$, $p > 0.05$, data not shown).

In another set of experiments, we included TTX in the external solution and applied a 100-msec preceding hyperpolarizing pulse, which resulted in a rebound LTS since sufficient hyperpolarization of the neuronal membrane caused deinactivation of T-channels. This protocol allowed us to measure the effects of 1-octanol on isolated LTS and input resistance in current-clamp experiments (Joksovic et al., 2006). On average, 10 μM 1-octanol decreased the amplitude of isolated LTS in nRT neurons for 35 ± 5% ($n = 5$, $p < 0.01$, data not shown). In contrast, average input resistance (R_{in}) was not

Molecular Pharmacology Fast Forward. Published on October 21, 2009 as DOI: 10.1124/mol.109.059931
This article has not been copyedited and formatted. The final version may differ from this version.

significantly affected in these cells (control 118 ± 2 MΩ, 1-octanol 162 ± 60 MΩ; n = 6, p > 0.05, data not shown). Somewhat greater 1-octanol-induced inhibition of isolated T-currents than LTS and associated burst firing may be related to better separation of T-currents from other ionic conductances in voltage-clamp experiments than current-clamp experiments, respectively.

Next we considered the possibility that potent inhibition of native T-current in nRT neurons by 1-octanol may be due to its direct interaction with a specific molecular isoform of T-channels that is expressed in this thalamic nucleus. Previous molecular studies using in-situ hybridization demonstrated that nRT has abundant transcripts for $Ca_V3.2$ (α1H) and $Ca_V3.3$ (α1I), but sparse $Ca_V3.1$ (α1G) isoforms of the pore-forming α1 subunit (Talley et al., 1999). Thus, we tested the sensitivity of recombinant rat $Ca_V3.3$ channels, which characteristically display slow inactivation kinetics similar to that of T-currents of native nRT cells (Joksovic et al., 2005a).

Figure 3A shows traces of inhibition of recombinant $Ca_V3.3$ current in HEK 293 cell with escalating concentrations of 1-octanol (30,100, 300, and 1000 μM). Figure 3B shows the time course from the same cell. Here, 1-octanol rapidly induced a reversible, almost complete concentration-dependent inhibition of $Ca_V3.3$ current. However, the black solid line representing the Hill plot of the average concentration-response curve in Figure 3C shows that this agent was more than 30-fold less potent in inhibiting recombinant $Ca_V3.3$ (IC_{50} 150 μM) than native nRT T-currents (solid gray line, IC_{50} 4 μM). The dashed black line in Figure 3C represents the Hill plot of the 1-octanol block of recombinant human $Ca_V3.2$ channels with an IC_{50} of 219 μM (from Todorovic et al., 2000). Most of our recordings with recombinant cells were done with intracellular solution containing 10 mM EGTA. Hence, we also examined the ability of 100 μM, 300 μM and 1000 μM 1-octanol to inhibit recombinant $Ca_V3.3$ currents with 1 mM intracellular

Molecular Pharmacology Fast Forward. Published on October 21, 2009 as DOI: 10.1124/mol.109.059931
This article has not been copyedited and formatted. The final version may differ from this version.

EGTA in order to provide more physiological concentrations of intracellular Ca^{2+} (Harney et al., 2006). However, in these experiments with low concentrations of EGTA we obtained similar potency of 1-octanol in inhibiting peak $Ca_V3.3$ current (fitted IC_{50} 176 ±1.0 μM, n 1.4 ± 0.1, n = 6 cells; data not shown). Thus, it appears that inhibitory effect of 1-octanol on recombinant $Ca_V3.3$ currents is not critically dependent on intracellular Ca^{2+} concentrations.

In contrast to the effect of 1-octanol on native T-current in nRT cells, traces on Figure 3A with 100 and 300 μM 1-octanol suggest that 1-octanol enhances the speed of macroscopic current inactivation. Thus, we fitted the decaying portion of the current with a single exponential function, finding that 1-octanol caused a significant increase in the $Ca_V3.3$ current inactivation rate as shown by a 3-fold decrease in inactivation time constant (τ) from 120 ± 20 ms to 41 ± 4 ms ($n = 8$, $p < 0.005$) for 100 μM 1-octanol (data not shown). In addition, 300 μM 1-octanol shifted the steady-state inactivation of $Ca_V3.3$ channels to hyperpolarized potentials by about 10 mV (Fig. 3D). In average, control steady-state inactivation was significantly shifted from -63.4 ± 3.4 mV to -72.7 ± 2.8 mV in the presence of 1-octanol (n=6 cells, $p<0.01$). We also examined the effects of 300 μM 1-octanol on I-V (Fig. 3E) and activation-voltage (Fig. 3F) relationships. The application of 1-octanol inhibited currents over the wide range of potentials, but there was no significant effect on midpoint of activation (control V_{50} -47.2 ± 1.7 mV, and -45.7 ± 3.1 mV in the presence of 1-octanol; n=6 cells, $p>0.05$).

We did biophysical studies to discern possible differences in the mechanisms of modulation of nRT and $Ca_V3.3$ T-type currents that could account for the higher potency of the inhibition of native currents by 1-octanol. Figure 4A shows a family of inward currents evoked by progressive depolarizing steps from -70 to -50 mV from a holding potential (V_h) of -90 mV in a representative nRT cell before (top traces) and during

Molecular Pharmacology Fast Forward. Published on October 21, 2009 as DOI: 10.1124/mol.109.059931
This article has not been copyedited and formatted. The final version may differ from this version.

(bottom traces) the application of 5 μM 1-octanol. Figure 4B depicts the average I-V curves from 5 nRT cells in experiments similar to those shown in Figure 4A. It is evident that 5 μM 1-octanol depressed peak current at all test potentials (V_t) more positive than -70 mV. From these experiments, we calculated the apparent voltage dependence of activation (Fig. 4C). The effect of 1-octanol on the midpoint of activation (V_{50}) in nRT neurons was shifted in depolarized potentials by about 4 mV (control -67.4 ±1.0 mV, 1-octanol -62.5 ± 2.0 mV; n=5, p>0.05). Importantly, 1-octanol had a significant voltage-dependent effect on steady-state inactivation, shifting midpoint of inactivation V_{50} to hyperpolarized potentials by about 12 mV (Fig. 4D). In average, in control conditions V_{50} occurred at – 87.8 ± 2.0 mV, and in the presence of 1-octanol in the same cells V_{50} was shifted to -100 ±1.0 mV (n=10, p<0.001). This was much like its effect in recombinant $Ca_V3.3$ channels.

Based on our results, we conclude that potent inhibition of native nRT currents by 1-octanol cannot be entirely explained either by a direct interaction with a particular known isoform of T-channels or specific biophysical features of channel block. Thus, we considered the possibility that 1-octanol interacts with second messengers in intact nRT neurons. Protein kinase C (PKC), an important signaling molecule, has been proposed as the putative target of general anesthesia (reviewed in Rebecci and Pentyla, 2002; Hemmings 1998). Previous data from other systems indicate that 1-octanol and related normal alcohols may either stimulate (Shen et al., 1999) or inhibit (Slater et al., 1993) the activity of PKC. Thus, we tested the ability of PKC activators and inhibitors to alter the baseline T-currents in nRT cells and to consequently affect the ability of 1-octanol to inhibit T-currents.

In these set of experiments, we first applied PKC activator, 300 nM phorbol 12-myristate 13-acetate (PMA) to nRT neurons. Figure 5A shows traces from a representative

Molecular Pharmacology Fast Forward. Published on October 21, 2009 as DOI: 10.1124/mol.109.059931
This article has not been copyedited and formatted. The final version may differ from this version.

neuron. PMA caused a small (about 17%) increase in baseline peak T-current without obvious changes in current kinetics. In a control experiment, an inactive form of PMA, 4α-PMA, at the same concentrations, had a minimal effect on baseline T-current (Fig. 5B). Overall, we found that 300 nM PMA increased baseline T-current in nRT cells by 16 ± 3% ($p < 0.001$, n=7), while 300 nM 4αPMA had no significant effect on baseline T-current in these cells (6 ± 5% increase, $p > 0.05$, n=5).

Our data is consistent with a modest stimulation of baseline T-current in nRT cells by PKC activation. However, since 1-octanol consistently inhibited T-currents in these cells, it is unlikely that its effects are mediated by PKC stimulation. We reasoned that if 1-octanol inhibits PKC in nRT cells, pharmacological or physiological inhibitors of PKC would also inhibit baseline T-current in nRT and interfere with the activity of 1-octanol to modulate this current. Molecular studies with in-situ hybridization indicate that both calcium-dependent and Ca^{2+}-independent isoforms of PKC have been expressed in the thalamus (Minami et al., 2000). To probe for the importance of Ca^{2+} ions in mediating 1-octanol inhibition of T-current in nRT cells, we used a high-affinity chelator of Ca^{2+} ions, BAPTA, which, at physiological pH, buffers Ca^{2+} approximately 100-fold faster than EGTA and can diminish cytosolic Ca^{2+} fast enough to suppress a biological response in the brain slices (Harney et al., 2006). Hence, we dialyzed BAPTA into cells *via* recording pipette solution at a high concentration of 10 mM. We used only nRT cells that had been dialyzed for at least 10 minutes in order to assure diffusion of BAPTA into dendritic regions. In the cells that still had significant T-currents under these recording conditions, we found that BAPTA completely abolished the ability of 10 μM 1-octanol to inhibit T-currents (2 ± 1% block, $p > 0.05$, n = 5). Figure 6A shows traces (left) and the time course of T-current (right) from a representative nRT neuron in the presence of BAPTA in internal solution. Furthermore, figure 6 B shows that acute application of 10 μM Go

Molecular Pharmacology Fast Forward. Published on October 21, 2009 as DOI: 10.1124/mol.109.059931
This article has not been copyedited and formatted. The final version may differ from this version.

6976, a specific Ca^{2+}-dependent PKC inhibitor, decreased baseline T-current amplitude about 40%, while subsequently co-applied 10 μM 1-octanol inhibited less than 10% of T-current amplitude. The histograms in Figure 6C summarize average data obtained when Go 6976 and 1-octanol were co-applied to the same cells. Overall, 1-octanol had no significant effect on baseline T-current in nRT cells treated with Go 6976 ($n = 5$, $p > 0.05$). In contrast, when we applied 10 μM Go 6976 on recombinant HEK 293 cells expressing $Ca_V3.3$ channels, there was no statistically significant effect on peak T-current amplitude (1 ± 6 % change, $n = 3$, $p>0.05$; data not shown). Thus, it appears that baseline native and recombinant T-currents are differently regulated and that the effects of 1-octanol on nRT currents are at least partly mediated by the inhibition of Ca^{2+}-dependent PKC pathway.

DISCUSSION

The major finding of our study is that the anesthetic alcohol 1-octanol induced a potent concentration-dependent inhibition (IC_{50} 4 μM) of native slowly inactivating T-currents and underlying burst firing in nRT neurons in intact brain slices. These effects could be important for the sedative and hypnotic action of anesthetic alcohols since the *in vitro* effect of 1-octanol in nRT neurons was well within the concentrations necessary to induce LRR in the tadpole anesthesia assay (Alifimoff et al., 1989). That assay is frequently used to estimate hypnotic properties of various drugs since its results generally correlate well with measures of anesthetic potency in mammals (Franks and Lieb, 1994). The inhibitory effect of 1-octanol on T-channel-dependent LTS and neuronal burst firing in nRT neurons (this study) and thalamo-cortical relay neurons (Soltesz et al., 1991; Llinas et al., 2007) could at least contribute to the inhibitory effect of anesthetics on neuronal firing in the thalamo-cortical sensory pathway. Such inhibitory effect on

thalamo-cortical circuitry is observed during *in vivo* anesthesia with other general anesthetics (Angel, 1991; Detsch et al., 2002). The effect of 1-octanol on LTS and burst firing of thalamic neurons in brain slices is similar to the effects of other classes of clinically used classical volatile anesthetics such as enflurane (Joksovic et al., 2005) and isoflurane (Ries and Puil, 1999). Hence, different classes of general anesthetics may have a common inhibitory effect on thalamo-cortical information transfer, which critically depends on the activity of T-channels. Our data further support the potential importance of T-channels as cellular targets for general anesthesia.

In at least two reports, potent inhibition of native T-currents by 1-octanol has been demonstrated. This was based on the findings that 1 μM 1-octanal blocked 75% of T-current in neonatal DRG cells (Scott et al., 1990), and 20 μM 1-octanol completely blocked T-currents in inferior olivary neurons (Llinas 1988). However, full-concentration response curves were not generated and the underlying mechanism of this potent inhibition of T-currents by 1-octanol was not further investigated in these studies.

Our study with recombinant T-channel isoforms expressed in HEK 293 cells indicates that these isoforms are inhibited by 1-octanol at up to 30-fold less potent concentrations than T-currents in native nRT cells. Binding of some drugs to inactivated states of the channel is an important property since it can provide pharmacological selectivity to their action. In particular, this mechanism can stabilize channel in inactive states and thus decrease availability of channel at physiological membrane potentials. We explore this hypothesis and found that 1-octanol significantly decreased availability of channel as evidenced by a hyperpolarizing shift of about 10 mV in steady-state inactivation curves of both recombinant $Ca_V3.3$ (Fig. 3) and native nRT T-currents (Fig. 4). While this is an important mechanism contributing to the preferential reduction of peak T-current at depolarized membrane potentials, it is unlikely that this could account

Molecular Pharmacology Fast Forward. Published on October 21, 2009 as DOI: 10.1124/mol.109.059931
This article has not been copyedited and formatted. The final version may differ from this version.

for a large difference in potency in native versus recombinant T-currents.

One possible reason for discrepancy in potency of T-current inhibition by 1-octanol between the native and recombinant cells could be different contents of membrane lipids. For example, it has been shown that membrane composition of lipid bilayers can drastically affect ability of anesthetics such as halothane and propofol (Hemmings and Adamo, 1994), as well as 1-octanol (Shen et al., 1999) to interact with lipid-bound regulatory domains of PKC. Furthermore, in our study the potent inhibitory effect of 1-octanol on T-current in nRT cells was critically dependent on constitutive Ca^{2+}-dependent PKC as shown by the fact that it was abolished with agents to inhibit it, as do the Ca^{2+} ion chelator BAPTA and Go 6976, a specific inhibitor of Ca^{2+}dependent isoforms of PKC. We also found that PMA induced a small but significant up-regulation of baseline T-current in nRT cells. Furthermore, Go 6976 blocked baseline T-current, strongly suggesting that endogenous PKC in nRT cells modulates T-current. In contrast, Go 6976 at the same concentration did not significantly affect recombinant $Ca_V3.3$ currents. In addition, changing intracellular Ca^{2+} buffering capacity with low concentrations of EGTA did not increase potency of 1-octanol in inhibiting recombinant $Ca_V3.3$ currents in HEK 293 cells. Thus, it appears that baseline T-current activity is differently regulated in native and recombinant cells. This is important, indicating a novel form of T-current modulation in nRT neurons by PKC. Earlier, we reported that nRT T-currents, LTS, and burst firing can be directly modulated by other endogenous agents such as reducing amino acid L-cysteine (Joksovic al., 2006) and S-nitrosothiols (Joksovic et al., 2007). Thus, different regulatory mechanisms regulate the expression of T-current in the finely tuned neuronal excitability of these cells.

Currently, the molecular basis for PKC modulation of T-current in nRT cells is not known. Several isoforms of PKC in neurons can be Ca^{2+} dependent (e.g., α, βI, βII, γ), or Ca^{2+} -independent (e.g., δ, ε, η, θ, μ) (Rebecchi and Pentyala, 2002). In-situ hybridization

Molecular Pharmacology Fast Forward. Published on October 21, 2009 as DOI: 10.1124/mol.109.059931
This article has not been copyedited and formatted. The final version may differ from this version.

studies have shown that PKC isoforms can be differentially expressed in the central nervous system, including the thalamus (Minami et al., 2000). Our results strongly suggest that Ca^{2+}-dependent PKC isoforms are tonically active in the up-regulation of T-current in nRT neurons and can be potently inhibited by 1-octanol. Recent studies with recombinant T-channel isoforms expressed in Xenopus oocytes (Park et al., 2006) and mammalian cells (Chemin et al., 2007) indicate that the amplitude of currents of all three known isoforms, $Ca_V3.2$, $Ca_V3.2$, and $Ca_V3.3$, may be enhanced up to 3-4-fold by PKC activation with prolonged incubation with PMA. Park et al. (2006) further showed that critical sites located in the I-II loop of the channel are responsible for the interaction of PMA and $Ca_V3.1$. However, the exact amino acid residues targeted by PKC action, presumably phosphorylation, have not been identified yet. It is interesting that the stimulatory effects of PKC upon T-current amplitude were strictly temperature-dependent in study using mammalian cells (Chemin et al., 2007), while similar effects were observed in oocytes at room temperature (Park et al., 2006). Interestingly, it appears that different T-current isoforms in two adjacent nuclei of the thalamus are differentially regulated by PKC. For example, PMA inhibits T-current in thalamo-cortical cells of ventrobasal nucleus that express predominantly $Ca_V3.1$ channels (Cheong et al., 2008), but enhances T-current in nRT cells that express $Ca_V3.2$ and $Ca_V3.3$ channels (our results). Extensive molecular studies in both recombinant and native cells are needed to decipher the precise mechanisms of the molecular interaction between T-channels, PKC and anesthetic alcohols.

In conclusion, we have demonstrated that 1-octanol potently inhibits native T-currents in nRT neurons likely by modulating Ca^{2+}-dependent PKC signaling. Moreover, T-channels in nRT neurons have a key function in thalamocortical oscillations, which in turn regulate physiological processes such as level of arousal and sleep, awareness, and sensory information transfer, as well as pathological processes such absence

Molecular Pharmacology Fast Forward. Published on October 21, 2009 as DOI: 10.1124/mol.109.059931
This article has not been copyedited and formatted. The final version may differ from this version.

seizures (Steriade, 2005). Thus, PKC modulation in nRT cells by anesthetic alcohols may contribute to the sedative, hypnotic, and anticonvulsant effects of general anesthesia.

Acknowledgements. We thank Dr. Edward Perez-Reyes for contribution of $Ca_V3.3$ HEK cells and Dr. Julie Sando for helpful discussion and critical comments.

REFERENCES

Alifimoff JK, Firestone LL and Miller KW (1998). Anaesthetic potencies of primary alkanols: implications for the molecular dimensions of the anaesthetic site. *Br J Pharmacol*. **96**(1**)**: 9-16.

Alkire MT, Haier RJ and Fallon JH (2000). Toward a unified theory of narcosis: brain imaging evidence for a thalamocortical switch as the neurophysiologic basis of anesthetic-induced unconsciousness. *Conscious Cogn* **9**: 370–386.

Angel A (1991). Adventures in anesthesia. *Exp Physiol* **76**, 1–38.

Chemin J, Mezghrani A, Bidaud I, Dupasquier S, Marger F, Barrère C, Nargeot J and Lory P (2007). Temperature-dependent modulation of CaV3 T-type calcium channels by protein kinases C and A in mammalian cells. *J Biol Chem* **282(45)**: 32710-8.

Cheong E, Lee S, Choi BJ, Sun M, Lee CJ, Shin HS (2008). Tuning thalamic firing modes via simultaneous modulation of T- and L-type Ca2+ channels controls pain sensory gating in the thalamus. *J Neurosci* **28(49)**:13331-40.

Detsch O, Kochs E, Siemers M, Bromm B and Vahle-Hinz C (2000). Differential effects of isoflurane on excitatory and inhibitory synaptic inputs to thalamic neurons in vivo. *Br J Anaesth* **89(2)**: 294-300.

Franks NP and Lieb WR (1994). Molecular and cellular mechanisms of general anesthesia. *Nature* **367**: 607–614.

Hamill OP, Marty E, Neher E, Sakmann B and Sigworth FJ (1981). Improved patch-clamp techniques for high-resolution current recording from cells and cell-free membrane patches. *Pfluegers Arch* **381**: 85-100.

Harney SC, Rowan M and Anwyl R (2006). Lon-term depression of NMDA receptor-mediated synaptic transmission is dependent on activation of metabotropic glutamate receptors and is altered to long-term potentiation by low intracellular calcium buffering. *J Neurosci* **26(4)**:1128-1132.

Herrington J and Lingle CJ (1992). Kinetic and pharmacological properties of low-voltage-activated Ca^{2+} current in rat clonal (GH3) pituitary cells. *J Neurophysiol* **68**: 213-232.

Hemmings HC Jr, Adamo AI (1994). Effects of halothane and propofol on purified brain protein kinase C activation. *Anesthesiology* **81(1)**:147-155.

Hemmings HC Jr (1998). General anesthetic effects on protein kinase C. *Toxicol Lett*. **100-101**: 89-95.

Joksovic PM, Brimelow BC, Murbartian J, Perez-Reyes E and Todorovic SM (2005a). Contrasting anesthetic sensitivities of slow T-type calcium channels of reticular thalamic neurons and recombinant $Ca_V3.3$ channels. *Br J Pharmacol* **144(1)**: 59-70.

Joksovic PM, Bayliss DA and Todorovic SM (2005b). Different kinetic properties of two T-type Ca^{2+} currents of rat reticular thalamic neurons and their modulation by enflurane. *J Physiol (London)* **566.1**: 1*25*-142*.*

Joksovic PM, Nelson MT, Jevtovic-Todorovic V, Patel MK, Perez-Reyes E, Campbell KP, Chen C-C and Todorovic SM (2006). $Ca_V3.2$ is the major molecular substrate for redox regulation of T-type Ca^{2+} channels in the rat and mouse thalamus. *J Physiol,* **574(2)**: 415-430.

Joksovic PM, Doctor A, Gaston B and Todorovic SM (2007). Functional regulation of T-type calcium channels by s-nitrosothiols in the rat thalamus. *J Neurophysiol* **97(4)**: 2712-21.

Llinás RR (1988). The intrinsic electrophysiological properties of mammalian neurons: insights into central nervous system function. *Science* **242(4886)**:1654-64.

Llinás RR, Choi S, Urbano FJ and Shin HS (2007). Gamma-band deficiency and abnormal thalamocortical activity in P/Q-type channel mutant mice. *Proc Natl Acad Sci U S A.* **104(45)**: 17819-24.

Llinas RR, Ribary U, Jeanmonod D, Kronberg E and Mitra PP (1998). Thalamocortical dysrhythmia: A neurological and neuropsychiatric syndrome characterized by magnetoencephalography. *Proc Natl Acad Sci U S A* **96(26)**: 15222-15227.

McCormick DA and Bal T (1997). Sleep and arousal: thalamocortical mechanisms. *Annu Rev Neurosci* **20**: 185-215.

Minami H, Owada Y, Suzuki R, Handa and Kondo H (2000). Localization of mRNAs for novel, atypical as well as conventional protein kinase C (PKC) isoforms in the brain of developing and mature rats. *J Mol Neurosci* **15(2)**: 121-35.

Murbartián J, Arias JM, Lee JH, Gomora JC and Perez-Reyes E (2002). Alternative splicing of the rat Ca(v)3.3 T-type calcium channel gene produces variants with distinct functional properties(1). *FEBS Lett* **528(1-3)**: 272-8.

Park JY, Kang HW, Moon HJ, Huh SU, Jeong SW, Soldatov NM and Lee JH (2006). Activation of protein kinase C augments T-type Ca2+ channel activity without changing channel surface density. *J Physiol* **577(Pt 2)**: 513-23.

Paxinos G and Watson C (1982). *The rat brain in stereotaxic coordinates*. Academic Press, Australia.

Perez-Reyes E (2003). Molecular physiology of low-voltage-activated T-type calcium channels. *Physiol Rev* **83**:117-161.

Rebecchi MJ and Pentyala SN (2002). Anaesthetic actions on other targets: protein kinase C and guanine nucleotide-binding proteins. *Br J Anaesth* **89(1)**: 62-78.

Ries CR and Puil E (1999). Mechanisms of anesthesia revealed by shunting actions of isoflurane on thalamocortical neurons. J Neurophysiol **81**: 1795-1801.

Rudolph U and Antkowiak B (2004). Molecular and neuronal substrates for general anaesthetics. *Nat Rev Neurosci* **5**: 709–720.

Scott RH, Wootton JF and Dolphin AC (1990). Modulation of neuronal T-type calcium channel currents by photoactivation of intracellular guanosine 5'-O(3-thio) triphosphate. *Neuroscience* **38(2)**: 285-94.

Slater SJ, Cox KJ, Lombardi JV, Ho C, Kelly MB, Rubin E and Stubbs CD (1993). Inhibition of protein kinase C by alcohols and anaesthetics. *Nature* **364(6432)**: 82-4.

Shen YM, Chertihin OI, Biltonen RL and Sando JJ (1999). Lipid-dependent activation of protein kinase C-alpha by normal alcohols. *J Biol Chem* **274(48)**: 34036-44, 1999.

Soltesz I, Lightowler S, Leresche N, Jassik-Gerschenfeld D, Pollard CE and Crunelli V (1991). Two inward currents and the transformation of low-frequency oscillations of rat and cat thalamocortical cells. *J Physiol* **441**:175-97.

Steriade M (2005). Sleep, epilepsy and thalamic reticular inhibitory neurons. *TINS* **28**: 317-324.

Takahashi K, Wakamori M and Akaike N (1989). Hippocampal CA1 pyramidal cells of rats have four voltage-dependent calcium conductances. *Neurosci Lett* **104(1-2)**: 229-34.

Talley EM, Cribbs LL, Lee J, Daud A, Perez-Reyes E and Bayliss DA (1999). Differential distribution of three members of a gene family encoding low-voltage-activated (T-type) calcium channels. *J Neurosci* **19(6)**: 1895-1911.

Todorovic SM and Lingle CJ (1998). Pharmacological properties of T-type Ca2+ current in adult rat sensory neurons: effects of anticonvulsant and anesthetic agents. *J Neurophysiol* **79**: 240-252.

Todorovic SM, Perez-Reyes E and Lingle CJ (2000). Anticonvulsants but not general anesthetics have differential blocking effects on different T-type current variants. *Mol Pharmacol* **58**: 98-108.

FOOTNOTES:

a) This work was supported by the grants from National Institute for Health [GM070726 and F31NS059190].

b) Reprint requests to Slobodan M. Todorovic, Department of Anesthesiology, University of Virginia Health System, 1 Hospital Drive, Mail Box 800710, Charlottesville, VA 22908-0710

Molecular Pharmacology Fast Forward. Published on October 21, 2009 as DOI: 10.1124/mol.109.059931
This article has not been copyedited and formatted. The final version may differ from this version.

FIGURE LEGENDS

Figure 1. Potent inhibition of native slowly inactivating T-currents in nRT neurons by 1-octanol.

A: Traces represent T-current elicited from V_h –90 mV to V_t –50 mV in a representative nRT neuron before and after (black lines), as well as during (gray line) the application of 10 μM 1-octanol. This resulted in depression of the current amplitude but had no apparent effect on the macroscopic kinetics of the current.

B: Symbols represents the time course of the effect on peak T-current before, during, and after the application of 1-octanol to the same cell as that in panel A. Depolarizing pulse was applied every 10 sec; the horizontal bar indicates time of the application. Inhibition of the peak current is gradual and partially reversible.

C: Concentration-response curve for T-current inhibition by 1-octanol. The solid symbols indicate the average of multiple determinations (n = 5 or more); vertical lines are ± S.E.M. (visible only if bigger than symbols). The solid line represents the best fit of the Hill equation. The fitted value for the curve is IC_{50} of 4 ± 1 μM, n = 1.6 ± 0.5; maximal fitted effect was constrained to 100% inhibition.

Figure 2. 1-octanol inhibits burst firing and LTS in nRT cells.

A. Representative traces recorded in current-clamp mode from an nRT neuron at a holding potential of -93 mV, indicated by the horizontal dashed line. LTS was evoked on injection of a small depolarizing pulse (duration,160 msec, amplitude 60 pA) and elicited a burst of 4 action potentials (APs). This burst was greatly diminished in the presence of 10 μM 1-octanol (one AP), but was completely recovered on washout of 1-octanol (four

Molecular Pharmacology Fast Forward. Published on October 21, 2009 as DOI: 10.1124/mol.109.059931
This article has not been copyedited and formatted. The final version may differ from this version.

APs). Bars indicate calibration. Holding potential was maintained by a constant injection of current *via* the recording electrode.

B. The histogram compares the number of AP spikes in control (4.8 ± 1.0) and in the presence of 1-octanol (3.0 ± 1.0). Asterisk indicates $p < 0.05$ (n = 6 cells, paired Student t-test). Vertical bars represent standard errors.

Figure 3. 1-octanol inhibits recombinant T-currents less potently than do native nRT T-currents.

A. Traces depict the inhibitory effect of escalating concentrations of 1-octanol on the amplitude of $Ca_V3.3$ current in a representative HEK 293 cell (V_h -90 mV, V_t -30 mV). A progressive increase in concentrations of 1-octanol leads to almost complete inhibition of T-current amplitude and apparent speeding of current inactivation kinetics.

B. Time course of T-current inhibition with 30, 100, 300, and 1,000 μM 1-octanol from the same cell as that in panel A. Horizontal bars indicate the duration of drug application. Note rapid onset and almost complete washout of the effect after each application. A depolarizing test pulse was applied every 20 seconds.

C. Symbols indicate the concentration-response curve for $Ca_V3.3$ T-type current inhibition by 1-octanol. The solid symbols indicate the average of multiple determinations (n = 5 or more); vertical lines are ± S.E.M. (visible only if bigger that symbols). The solid black line represents the best fit of the Hill equation for $Ca_V3.3$. The fitted value for the curve is IC_{50} of 149.4 ± 35.6 μM, n = 1.3 ± 0.4; maximal fitted effect was constrained to 100% inhibition. The solid gray line is the same as that in Figure 1C, indicating that native T-current in nRT cells is 30-fold more potently inhibited by 1-octanol than recombinant $Ca_V3.3$ current. The dashed line represents the best fit of the Hill equation

Molecular Pharmacology Fast Forward. Published on October 21, 2009 as DOI: 10.1124/mol.109.059931
This article has not been copyedited and formatted. The final version may differ from this version.

for $Ca_V3.2$ current (from Todorovic et al., 2000) yielding an IC_{50} of 219 μM, n = 1.4; curve fit was constrained to 100% inhibition.

D. The steady-state inactivation kinetics of T-currents in $Ca_V3.3$-transfected HEK cells were examined by paired-pulse protocols at different conditioning potentials. Double-pulse protocols to -30 mV were used to elicit T-currents, separated by 3.5-second prepulse to potentials ranging from -110 to -40 mV before (filled symbols) and during (open symbols) the application of 300 μM 1-octanol. The data were best fitted with the Boltzmann equation, yielding V_{50} of -64.5±0.3 mV (k = 7.4 ± 0.3 mV) in control and -74.4 ± 0.4 mV (k = 8.0 ± 0.3 mV) in the presence of 1-octanol (n = 5 cells).

E. The average I-V relationships before (●) and during (○) the application of 300 μM 1-octanol. Currents were elicited by progressing from -80 mV to 30 mV in 5-mV increments from a holding potential of -90 mV (n = 6 cells). Note the depression of the current amplitude at most potentials and the slight shift of the I-V curve to the right in the presence of 1-octanol.

F. Normalized conductance in whole-cell recordings from current-voltage experiments depicted in panel E of this figure. The average half-conductance (V_{50}) was in control -47.2 ± 0.4 mV (k = 3.2 ± 0.3 mV) and in the presence of 1-octanol was -40.4 ± 0.4 mV (k = 7.1 ± 0.4 mV). Fits were done using the Boltzmann equation. The estimated reversal potential was taken to be 50 mV.

Figure 4. The effects of 1-octanol on the kinetic properties of T-currents in nRT neurons.

A. A family of raw T-current traces in a representative nRT cell elicited with test potentials from -70 to -50 mV in 5-mV increments from a holding potential of -90 mV in

Molecular Pharmacology Fast Forward. Published on October 21, 2009 as DOI: 10.1124/mol.109.059931
This article has not been copyedited and formatted. The final version may differ from this version.

control conditions (top traces) and in the presence of 5 μM 1-octanol in external solution (bottom traces). Bars indicate calibration.

B. The average I-V relationships before (●) and during (○) the application of 5 μM 1-octanol. Currents were elicited by progressing from -80 mV to -20 mV in 5-mV increments from a holding potential of -90 mV (n = 5 cells). Note the depression of the current amplitude at most potentials and the slight shift of the I-V curve to the right in the presence of 1-octanol.

C. Normalized conductance in whole-cell recordings from current-voltage experiments depicted in panel B of this figure. 1-octanol shifted half-conductance (V_{50}) to the right from -67.2 ± 0.4 mV (k = 2.4 ± 0.4 mV) in control to -63.8 ± 2.5 mV (k = 5.7 ± 2.6 mV). Fits were done using the Boltzmann equation.

D. The steady-state inactivation kinetics of T-currents in nRT neurons were examined by paired-pulse protocols at different conditioning potentials. Double-pulse protocols to -50 mV were used to elicit T-currents separated by 3.5-sec prepulse to potentials ranging from -110 to -50 mV in 5-mV increments before (filled symbols) and during (open symbols) the application of 1-octanol. The data were best fitted with the Boltzmann equation, yielding V_{50} of -88.0 ± 0.2 mV (k = 5.0 ± 0.1 mV**)** in control and -99.6 ± 0.2 mV (k=3.7 ± 0.2 mV) in the presence of 1-octanol (n = 10 cells).

Figure 5. PMA enhances the amplitude of nRT T-current.

A. This panel shows representative traces of peak T-type current amplitudes (V_h –90 mV, V_t –50 mV) before (control, black trace) and during applications of 300 nM PMA (gray trace). PMA application increased T-current amplitude about 17%.

Molecular Pharmacology Fast Forward. Published on October 21, 2009 as DOI: 10.1124/mol.109.059931
This article has not been copyedited and formatted. The final version may differ from this version.

B. This panel depicts representative traces of peak T-current amplitudes (V_h –90 mV, V_t –50 mV) before (control, black trace) and during applications of 300 nM 4αPMA (gray trace). Application of 4αPMA had very little effect on T-current amplitude.

Figure 6. Calcium-dependent PKC is the possible cellular target of 1-octanol inhibition of T-current in nRT cells.

A. This panel illustrates traces (left) and time course (right) from a representative nRT cell dialyzed with 10 mM BAPTA. Note that 10 μM 1-octanol had little effect on T-current amplitude or current kinetics.

B. Traces (left) and time course (right) from another nRT cell. Note that 10 μM 1-octanol was applied to this cell after it had been exposed to 10 μM Go 6976, a specific Ca^{2+}-dependent PKC inhibitor. By itself, Go 6976 inhibited about 40% of baseline T-current but, with 1-octanol, the two together inhibited about 48% of the current.

C. The average data from experiments similar to those presented in panel B indicate that Go 6976 reduced peak T-current to 66 ± 3% of the baseline level ($p < 0.001$, $n = 5$) but that co-application of 10 μM 1-octanol to the same cells did not significantly affect the new baseline (60 ±1%, $p > 0.05$). n.s indicates $p > 0.05$.

Molecular Pharmacology Fast Forward. Published on October 21, 2009 as DOI: 10.1124/mol.109.059931
This article has not been copyedited and formatted. The final version may differ from this version.

nRT Figure 1

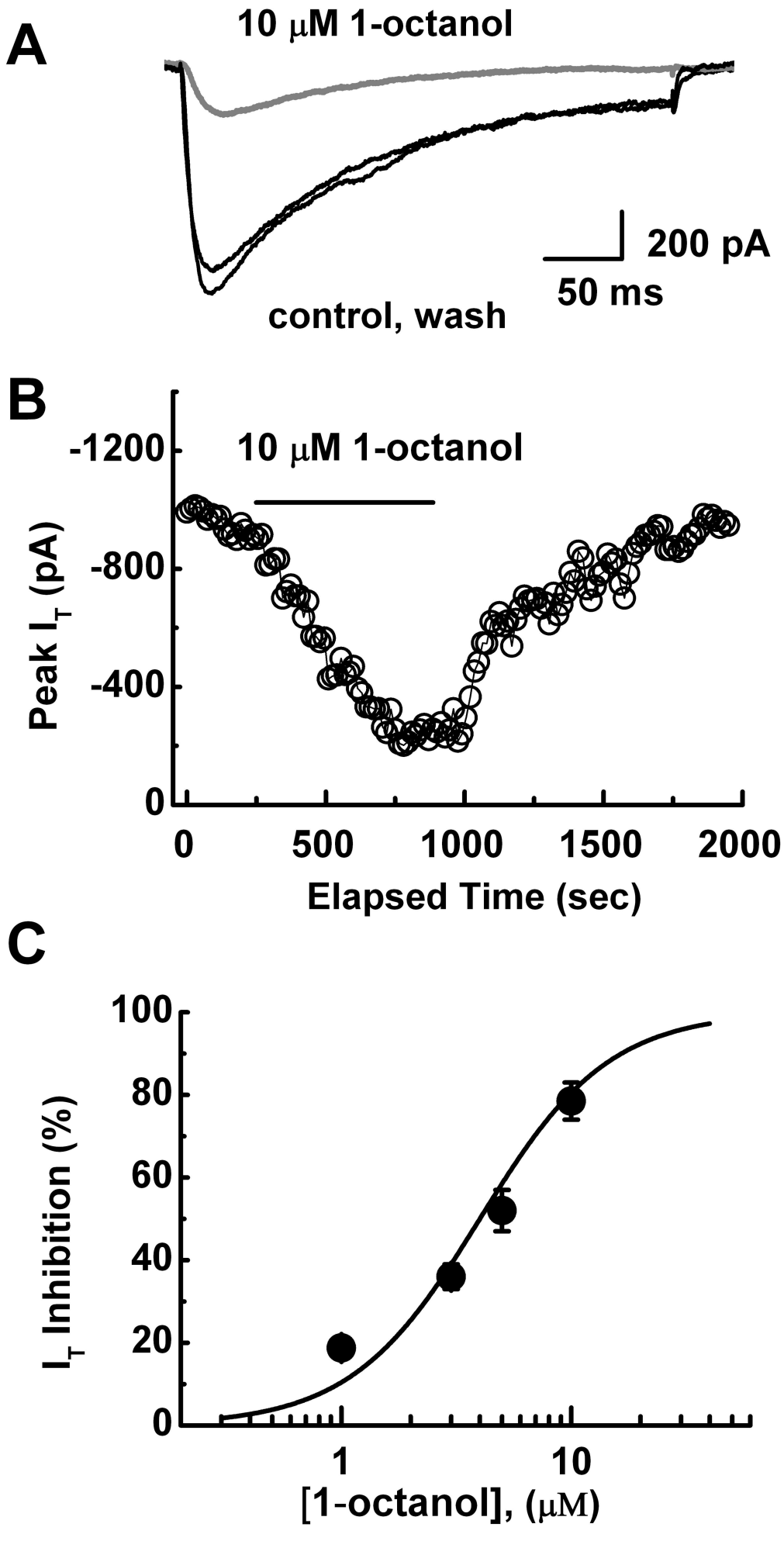

Molecular Pharmacology Fast Forward. Published on October 21, 2009 as DOI: 10.1124/mol.109.059931
This article has not been copyedited and formatted. The final version may differ from this version.

nRT

Figure 2

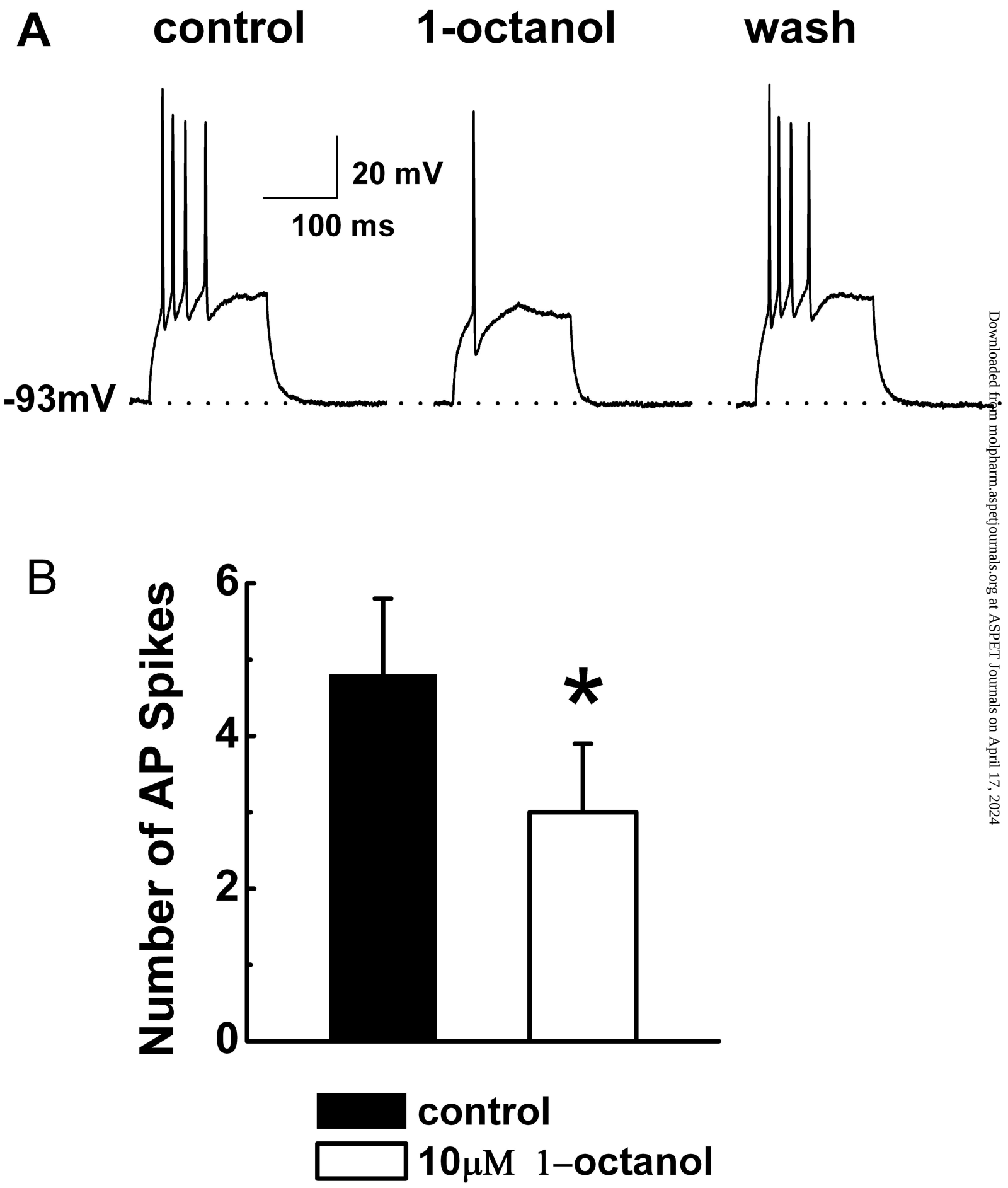

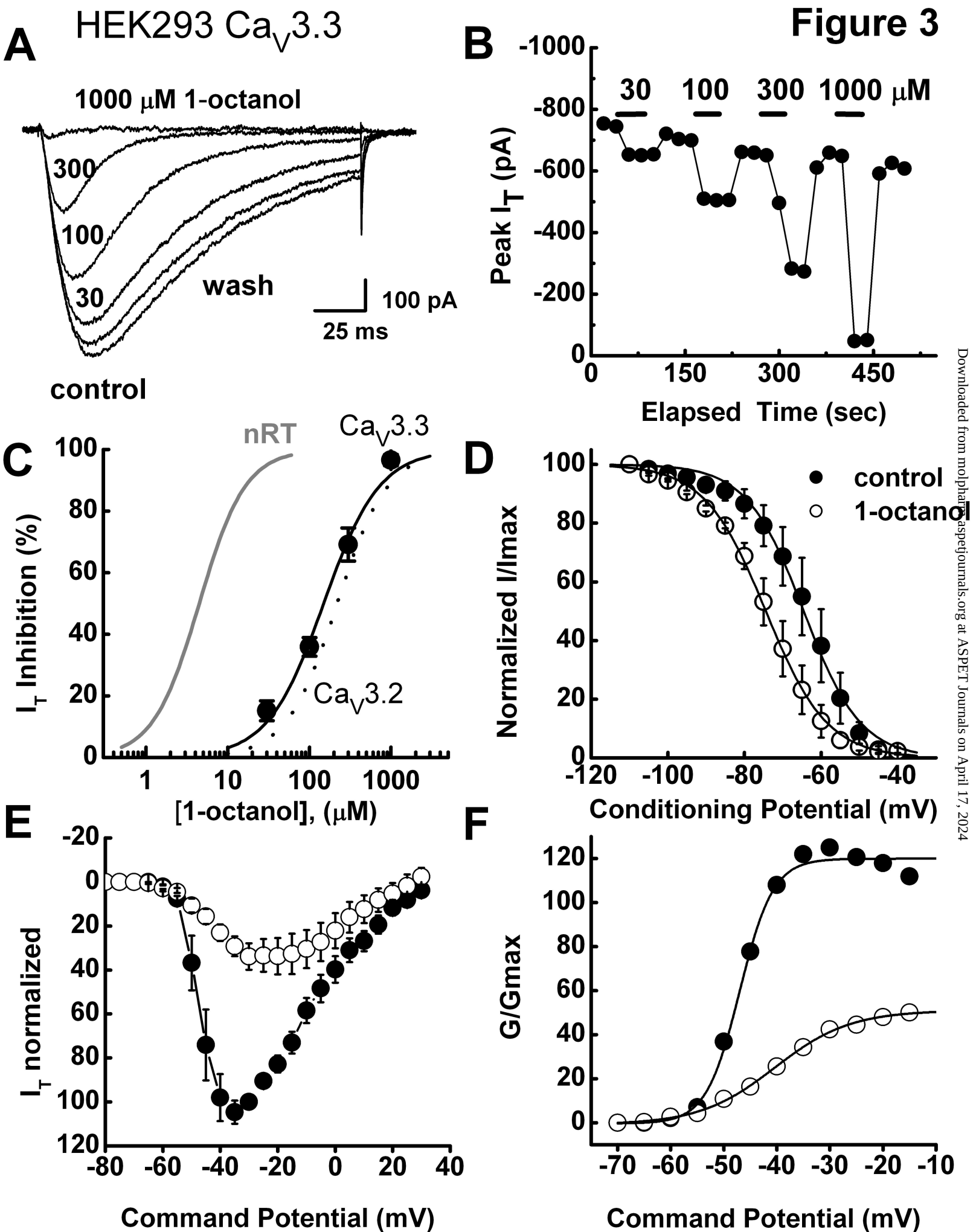

Molecular Pharmacology Fast Forward. Published on October 21, 2009 as DOI: 10.1124/mol.109.059931
This article has not been copyedited and formatted. The final version may differ from this version.

Figure 4

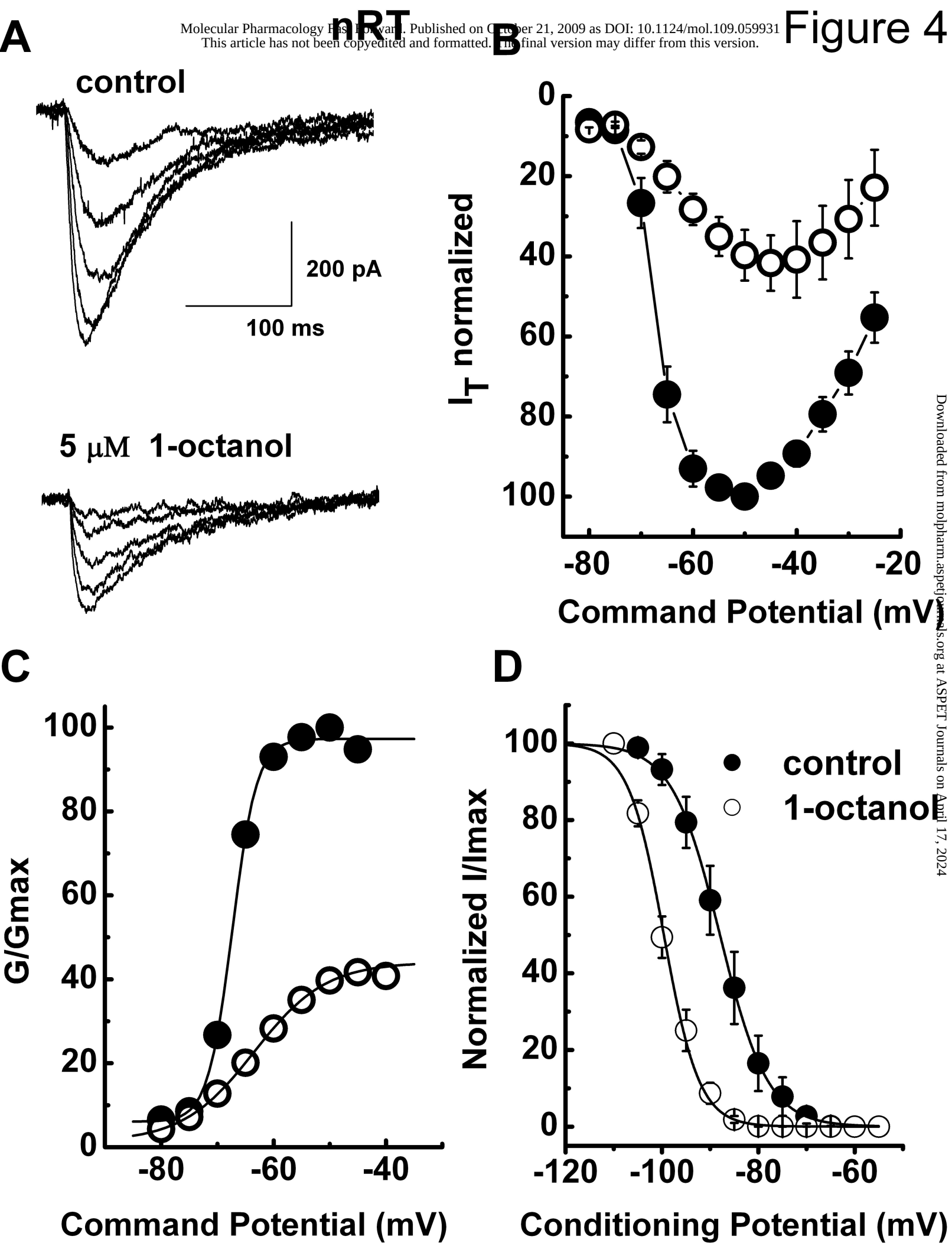

Molecular Pharmacology Fast Forward. Published on October 21, 2009 as DOI: 10.1124/mol.109.059931
This article has not been copyedited and formatted. The final version may differ from this version.

Figure 5

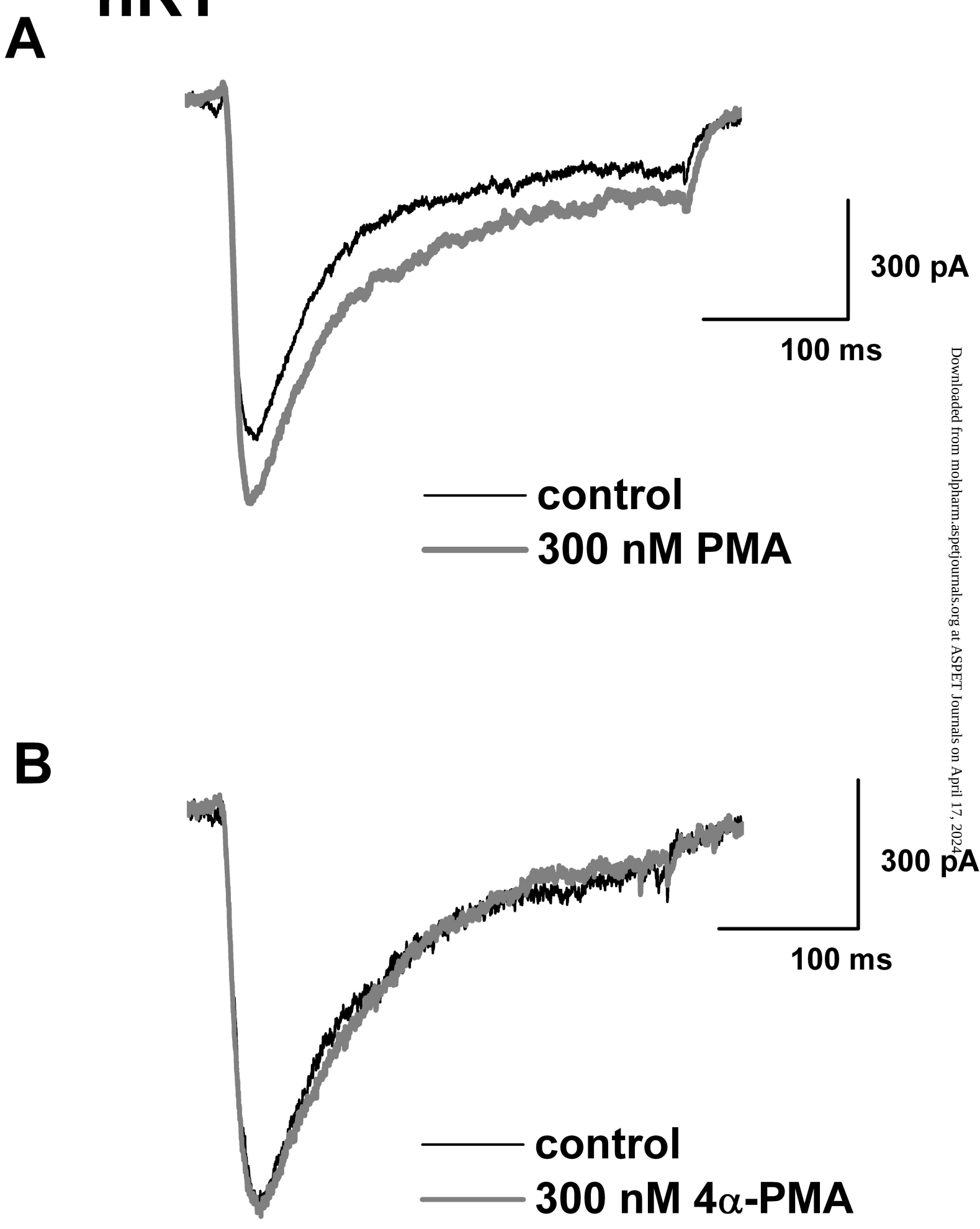

Molecular Pharmacology Fast Forward. Published on October 21, 2009 as DOI: 10.1124/mol.109.059931
This article has not been copyedited and formatted. The final version may differ from this version.

Figure 6